Electronic Supplementary Material (ESI) for Chemical Communications.

Contents

General Information

All the purchased reagents were of standard quality and used without further purification. Dichloromethane and xylene (super dehydrated grade) used as reaction solvent were purchased from Kanto Chemical Co., Inc. All the reactions were carried out under N_2 atmosphere. 4-Bromophenylferrocene (**3**) was synthesized according to the literature.[S1] Flash chromatography was performed with a Biotage Isorela medium pressure liquid chromatography (MPLC) system and a SNAP Sfär flash silica gel cartridge (Biotage). ^{1}H and ^{13}C NMR spectra were recorded by a Varian 400-MR FT-NMR spectrometer. Low- and high-resolution fast atom bombardment (FAB+) mass spectra (MS) were obtained on a JEOL JMS-700 mass spectrometer. UV-Vis-NIR absorption spectra were obtained with a JASCO V-670 spectrometer with a UNISOKU CoolSpeK cryostat. Cyclic voltammetry and differential pulse voltammetry were measured in BAS Electrochemical Analyzer ALS Model 612B.

[S1] C. A. Fleckenstein, H. Plenio, *Adv. Synth. Catal*. 2006, **348**, 1061.

Synthetic Details

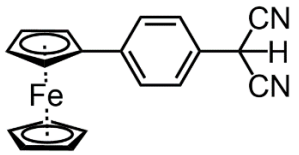

2_H

2_H: Malononitrile (79.2 mg, 1.20 mmol), NaO^{t}Bu (290 mg, 3.0 mmol) and dry xylene (15.0 mL) were stirred for 1 h at room temperature. 4-Bromophenylferrocene **3** (342 mg, 1.00 mmool) and $Pd(PPh_3)_2$ Cl_2 (35.1 mg, 0.05 mmol) were added and the reaction mixture was stirred at 160 °C for 5 h. The reaction mixture was cooled down to room temperature and quenched by 10% HCl aq. solution. The product was extracted into diethyl ether and the organic layer was washed with brine. The organic layer was dried over Na_2SO_4 and the solvent was removed by rotary evaporation. The crude product was chromatographed on silica gel (hexane/CH_2Cl_2 = 2/1, R_f = 0. 50) to afford **2** (193.8 mg, 59%) an orange powder.

^{1}H NMR (400 MHz, $CDCl_3$): δ = 4.05 (s, 5H, Fc), 4.38 (t, J = 1.9 Hz, 2H, Fc), 4.67 (t, J = 1.9 Hz, 2H, Fc), 5.03 (s, 1H, CH), 7.40 (d, J = 8.0 Hz, 2H, Ph), 7.57 (d, J = 8.0 Hz, 2H, Ph); ^{13}C NMR (100 MHz, $CDCl_3$): δ = 27.87, 66.74, 69.68, 69.79, 83.00, 111.81, 122.89, 127.24, 127.27, 142.53; HRMS (FAB+, Matrix = 3-Nitrobenzyl alcohol) m/z calcd for $C_{19}H_{14}FeN_2$: 326.0506 found 326.0505 (Δ = −0.3 ppm). m.p. 164–167 ºC.

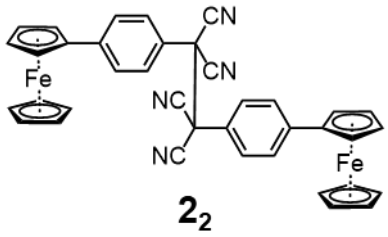

2₂

2₂: In a two-necked flask, **2H** (99 mg, 0.30 mmol) was placed and dichloromethane (10.0 ml) was added under nitrogen atmosphere. To the flask, a solution of $K_3[Fe(CN)_6]$ (1.50 g, 4.50 mmol) and KOH (84.2 mg, 1.50 mmol) in water (15.0 ml) was added and the mixture was stirred for 1 h at room temperature. The product was extracted into CH_2Cl_2 and the organic layer was washed with brine. The organic layer was dried over Na_2SO_4 and the solvent was removed by rotary evaporation. The crude product was chromatographed on silica gel (hexane/CH_2Cl_2 = 1/1, R_f = 0. 50) to afford **2₂** (93 %) as an orange powder. m.p. 192–194 ºC.

^{1}H NMR (400 MHz, $CDCl_3$): δ= 4.05 (s, 10H), 4.43 (s, 4H), 4.70 (s, 4H), 7.36 (d, J = 8.0 Hz, 4H), 7.53 (d, J = 8.0 Hz, 4H); ^{13}C NMR (100 MHz, $CDCl_3$): δ=52.75, 66.89, 69.97, 70.26, 81.71, 110.55, 120.98, 126.42, 128.34, 145.23; HRMS (FAB+, Matrix = 3-Nitrobenzyl alcohol) m/z calcd for $C_{19}H_{13}FeN_2$: 325.0428; found 325.0432 (Δ = +1.1 ppm)

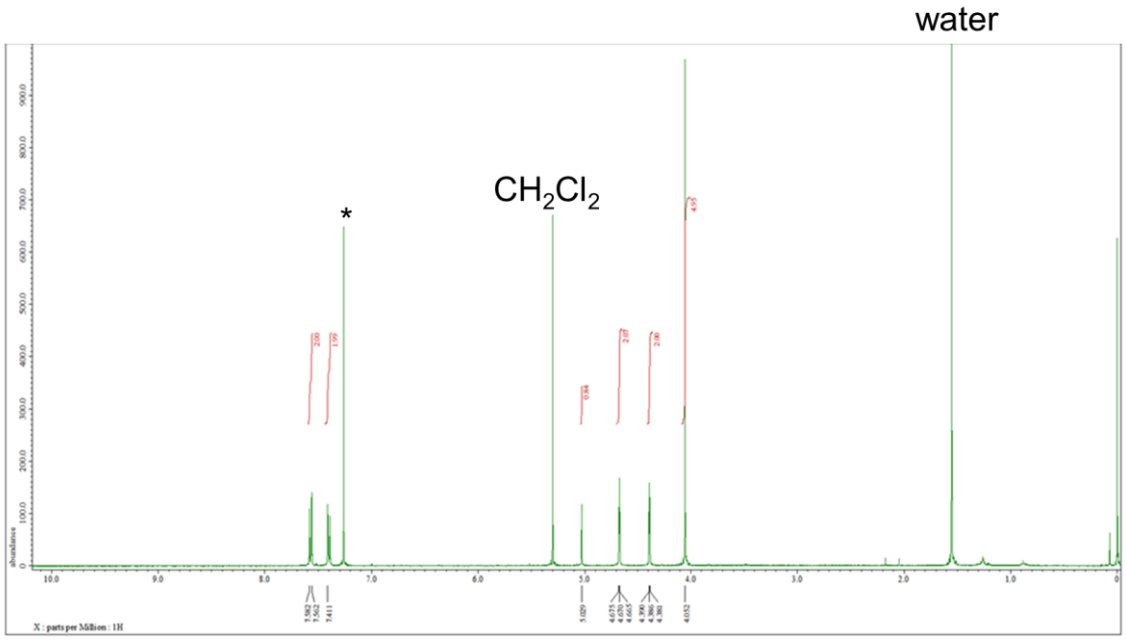

Figure S1. ^{1}H NMR spectrum of **2H** in chloroform-d_1. Asterisk denotes the solvent residual peak.

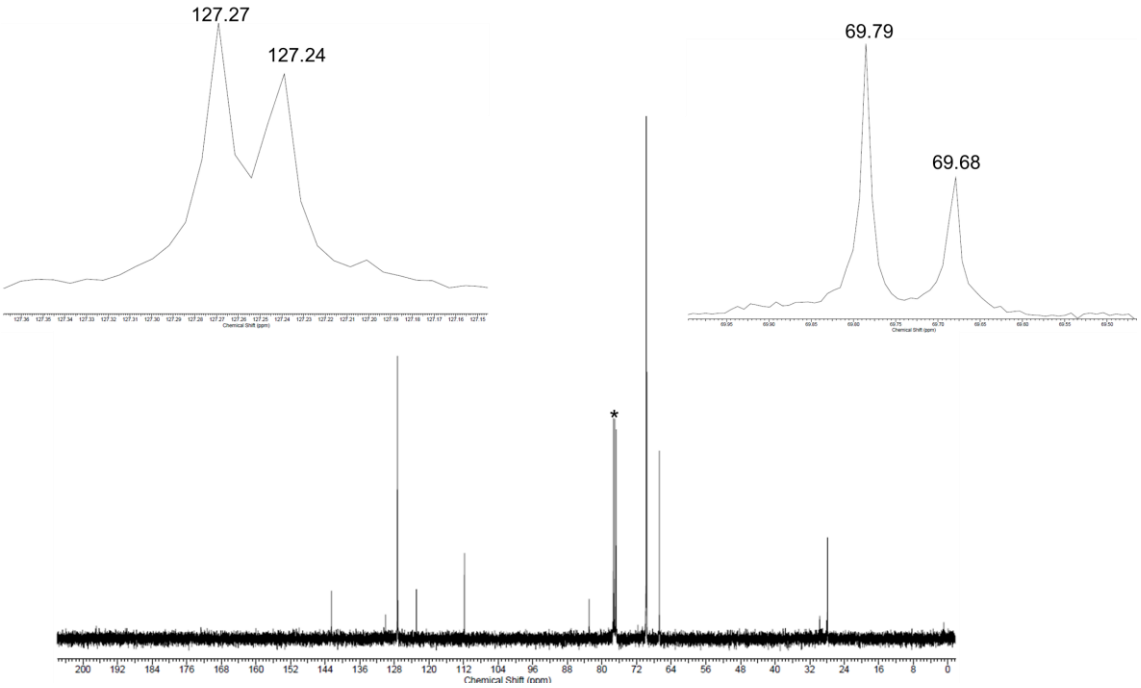

Figure S2. ^{13}C NMR spectra of **2H** in chloroform-d_1. Asterisk denotes the solvent residual peak.

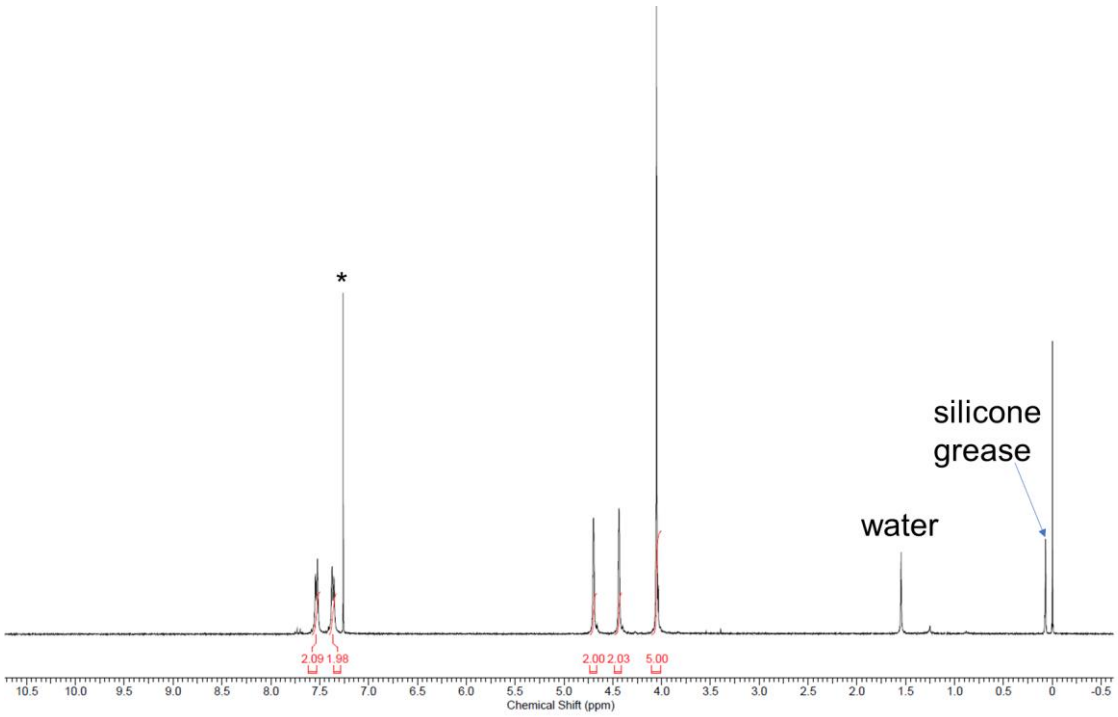

Figure S3. ^{1}H NMR spectrum of **2₂** in choroform-d_1. Asterisk denotes the solvent residual peak.

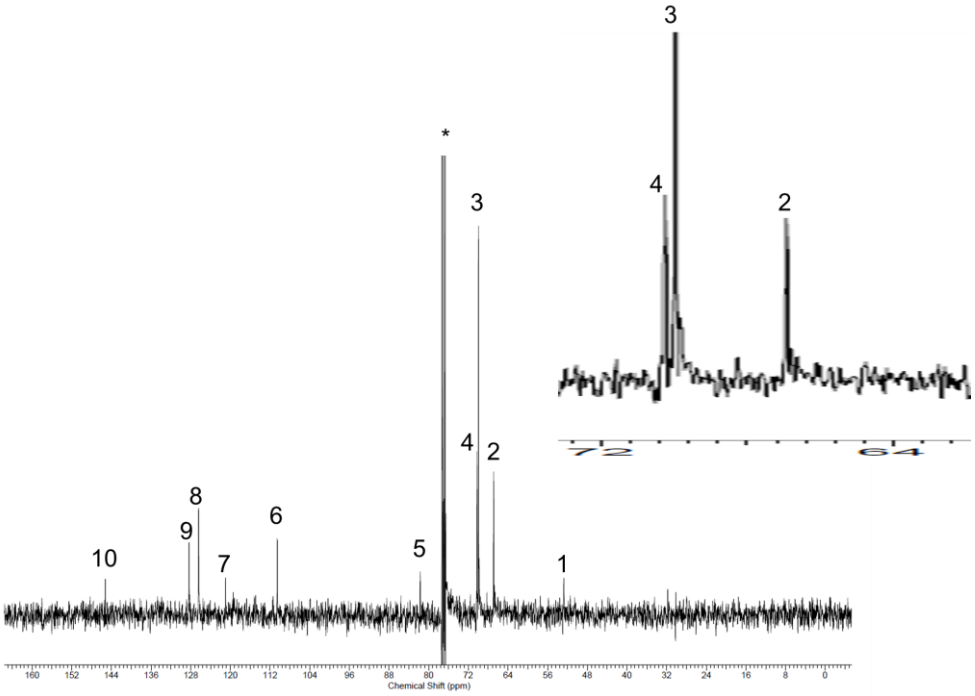

Figure S4. ^{13}C NMR spectrum of **2₂** in choroform-d_1. Asterisk denotes the solvent residual peak.

X-ray Crystallography

The single crystals of $\mathbf{2_H}$ and $\mathbf{2_2}$ were obtained by the slow evaporation of dichloromethane/hexane and chloroform/hexane solution, respectively. Data collections were performed on a Rigaku R-AXIS RAPID diffractometer with Mo-Kα radiation at 173 K. The hydrogen atoms were refined using the riding model. All the calculations were performed by using CrystalStructure crystallographic software package,[S2] except for refinement, which was performed by using SHELXL Version 2017/1.[S3] The CIF file has been deposited on the Cambridge Crystallographic Data Centre (CCDC), under deposition numbers CCDC 2129586 ($\mathbf{2_H}$) and 2129587 ($\mathbf{2_2}$).

[S2] CrystalStructure 4.3: Crystal Structure Analysis Package, Rigaku Corporation (2000-2018). Tokyo 196-8666, Japan.

[S3] G. M. Sheldrick, Acta Cryst. A **2008**, *64*, 112.

Table S1: X-ray crystallographic data for **2H** (CCDC 2129586).

empirical formula	$C_{19}H_{14}N_2Fe$
formula weight	326.18
T [˚C]	–100
λ [Å]	0.71075
crystal system	monoclinic
space group	$P2_1/n$
Z	4
a [Å]	15.4417(9)
b [Å]	5.8159(3)
c [Å]	16.2351(8)
β [˚]	97.864(7)
V [Å^3]	1444.31(13)
ρ_{calcd} [g cm^{-3}]	1.500
collected data	13290
unique data / R_{int}	3281/0.0217
no. of parameters	255
goodness-of-fit[a]	1.051
$R1$ ($I > 2\sigma$), $wR2$ (all reflections)[b]	0.0323, 0.0797
residual density [e Å^{-3}]	0.57/–0.26

[a] GOF = $\left\{\sum\left[w\left(F_0^2 - F_c^2\right)^2\right]/(n-p)\right\}^{1/2}$, where n and p denote the number of data and parameters.

[b] $R1 = \sum\left(\|F_0\| - \|F_c\|\right)/\sum\|F_0\|$ and $wR2 = \left\{\sum\left[w\left(F_0^2 - F_c^2\right)^2\right]/\sum\left[w\left(F_0^2\right)^2\right]\right\}^{1/2}$ where $w = 1/\left[\sigma^2\left(F_0^2\right) + (a\cdot P)^2 + b\cdot P\right]$ and $P = \left[\left(\text{Max}; 0, F_0^2\right) + 2\cdot F_c^2\right]/3$.

Table S2: X-ray crystallographic data for **2₂** (CCDC 2129587).

empirical formula	$C_{38}H_{26}N_4Fe_2$
formula weight	650.34
T [˚C]	–100
λ [Å]	0.71075
crystal system	monoclinic
space group	$P2_1/c$
Z	2
a [Å]	17.371(2)
b [Å]	10.1537(16)
c [Å]	8.4136(15)
β [˚]	103.231(7)
V [Å^3]	1444.6(4)
ρ_{calcd} [g cm^{-3}]	1.495
collected data	13132
unique data / R_{int}	3290/0.1272
no. of parameters	212
goodness-of-fit[a]	1.237
$R1$ ($I > 2\sigma$), $wR2$ (all reflections)[b]	0.1597, 0.1469
residual density [e Å^{-3}]	3.340/–2.710

[a] GOF = $\left\{\sum\left[w\left(F_0^2 - F_c^2\right)^2\right]/(n-p)\right\}^{1/2}$, where n and p denote the number of data and parameters.

[b] $R1 = \sum\left(\|F_0\| - \|F_c\|\right)/\sum\|F_0\|$ and $wR2 = \left\{\sum\left[w\left(F_0^2 - F_c^2\right)^2\right]/\sum\left[w\left(F_0^2\right)^2\right]\right\}^{1/2}$ where $w = 1/\left[\sigma^2\left(F_0^2\right) + (a\cdot P)^2 + b\cdot P\right]$ and $P = \left[\left(\text{Max}; 0, F_0^2\right) + 2\cdot F_c^2\right]/3$.

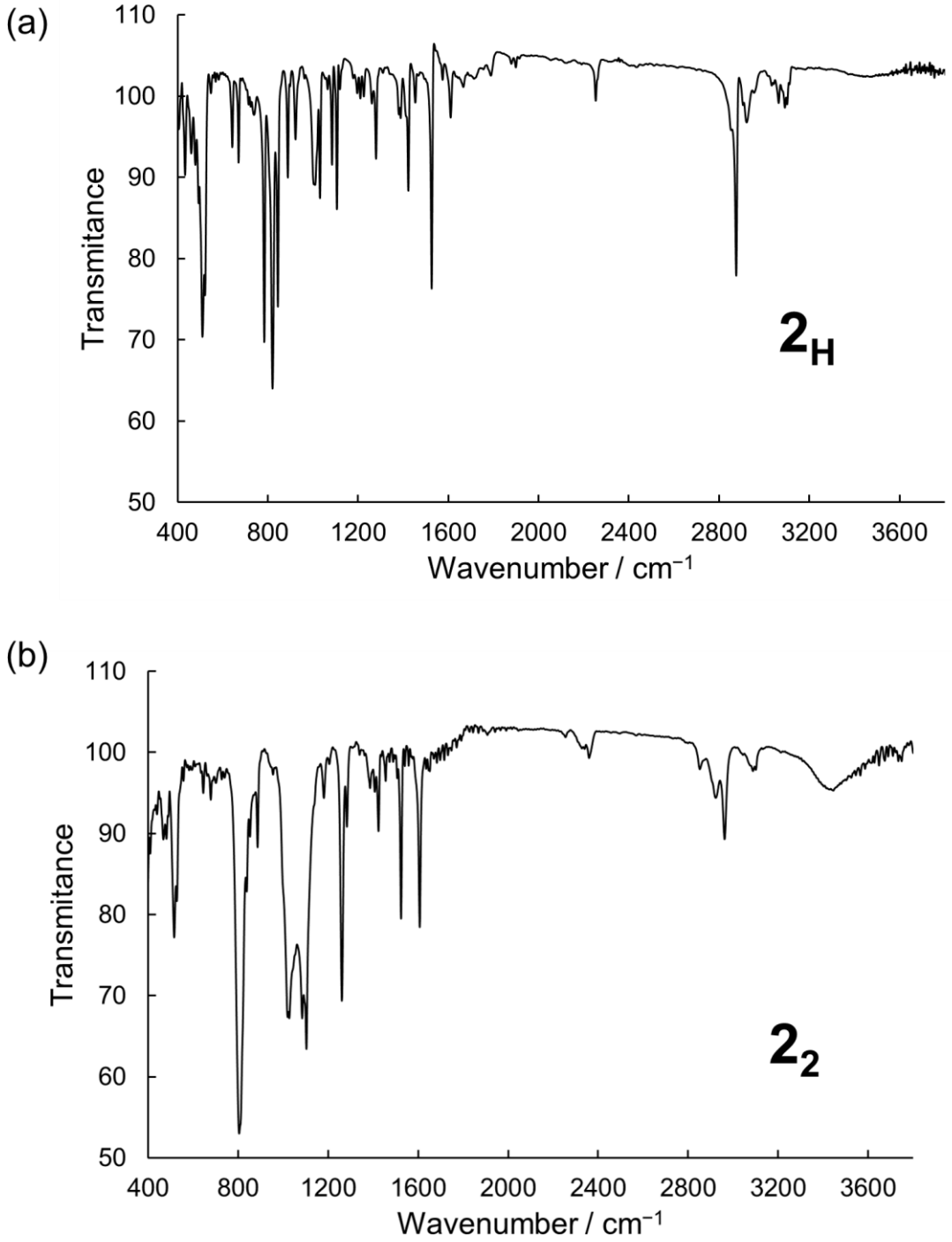

Figure S5. IR spectra of (a) $\mathbf{2_H}$ and (b) $\mathbf{2_2}$ in KBr pellets.

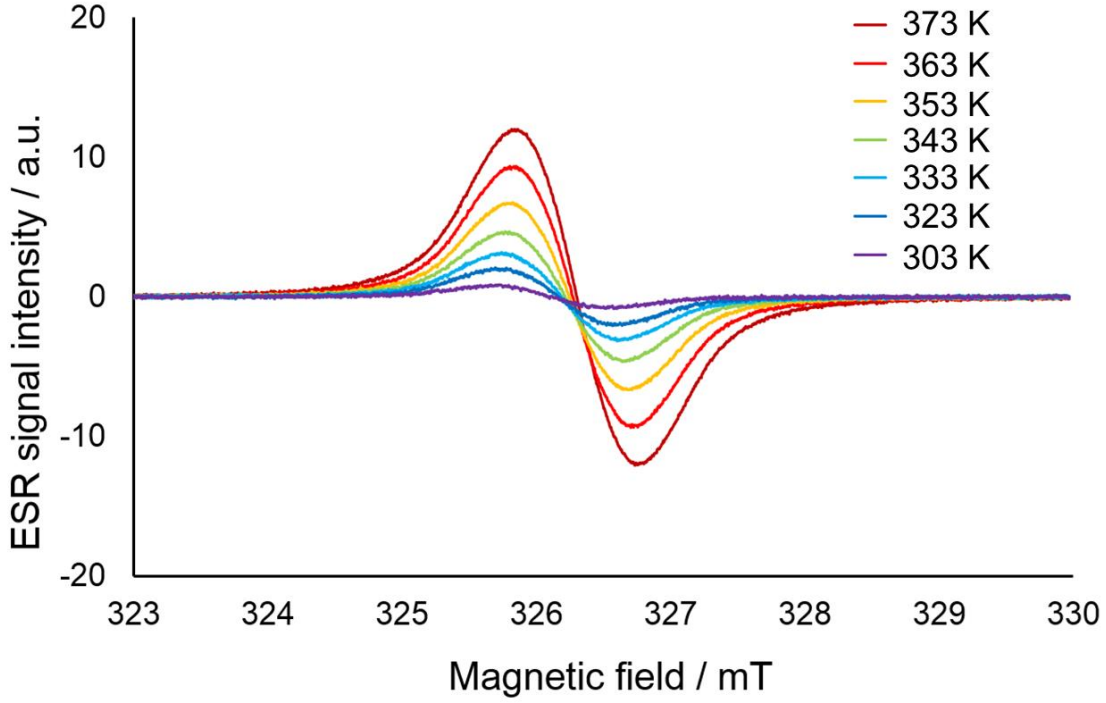

Figure S6. Temperature dependence of ESR spectra of $\mathbf{2}_2$ in toluene.

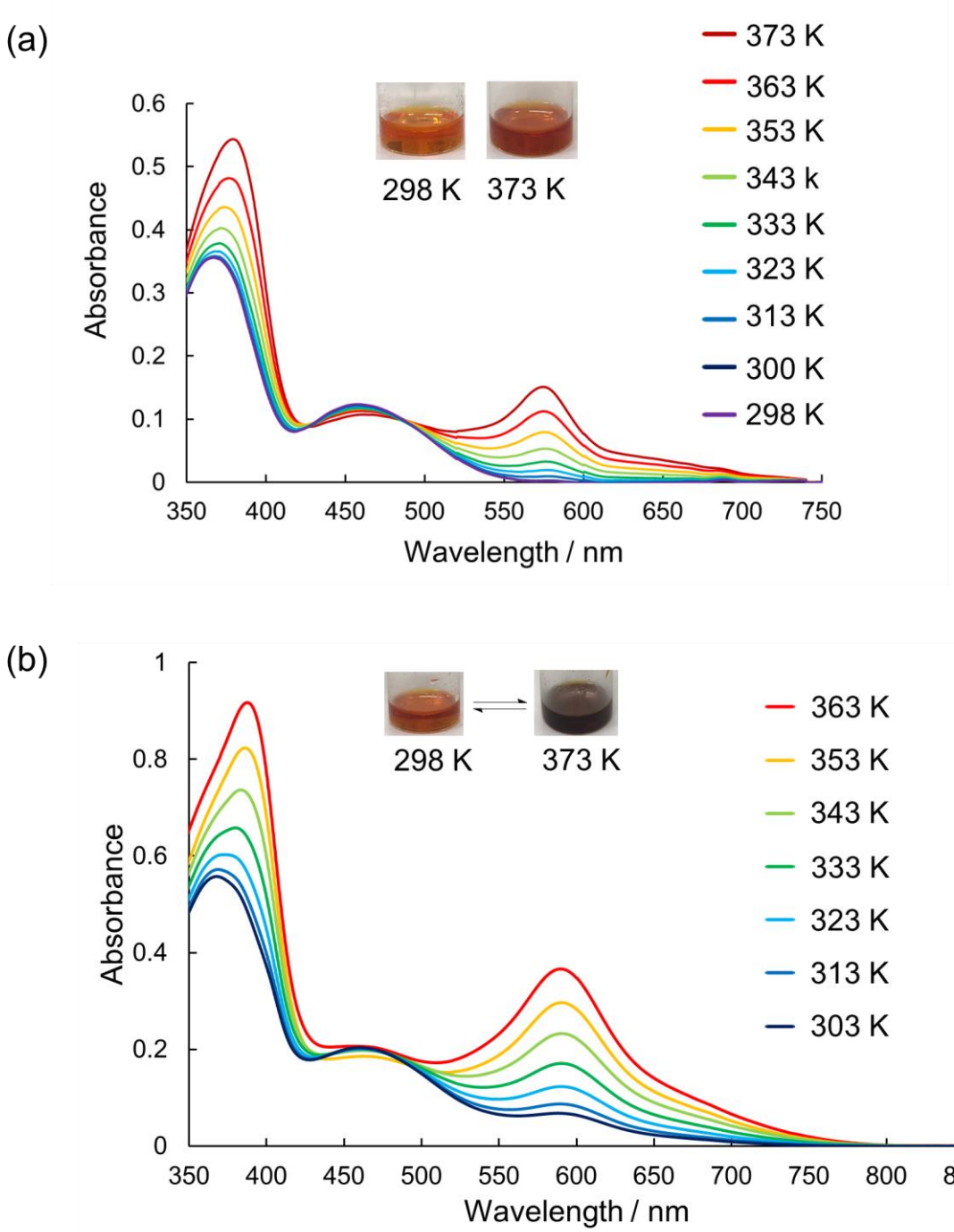

Figure S7. Temperature dependence of the UV-Vis absorption spectra and the colour change of **2₂** in (a) toluene and (b)benzonitrile (1×10^{-4} M).

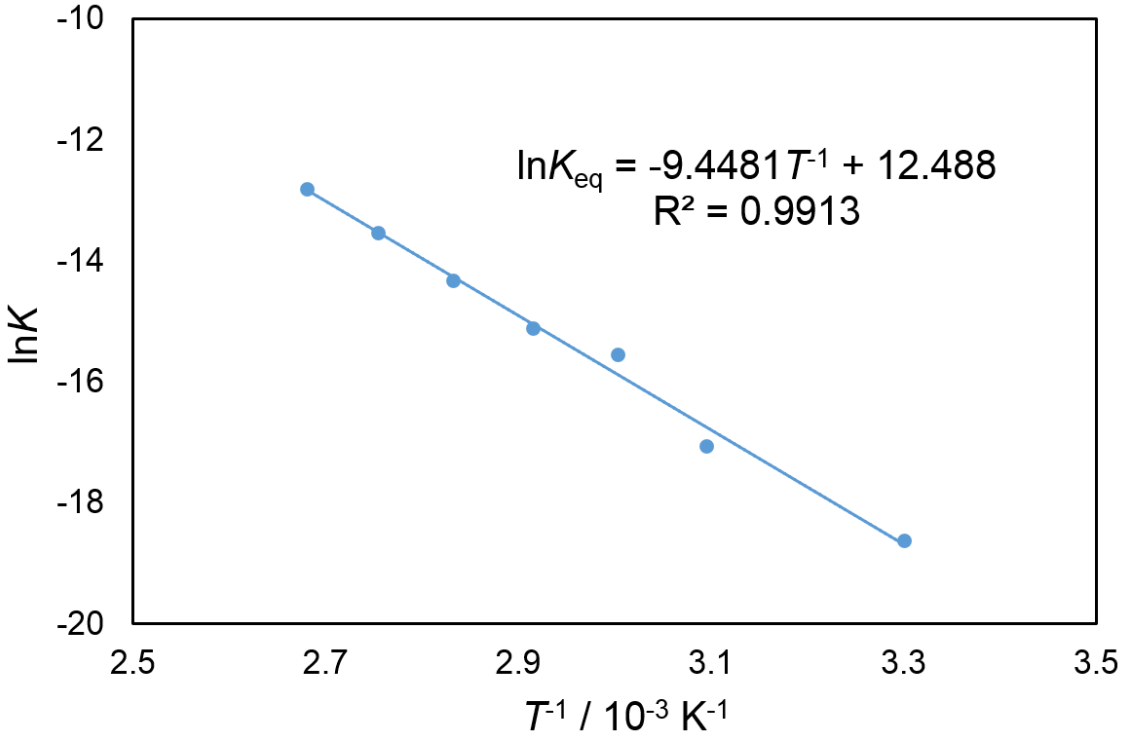

Figure S8. van't Hoff plot (ln K_{eq} vs T^{-1}) for **2₂** in toluene.

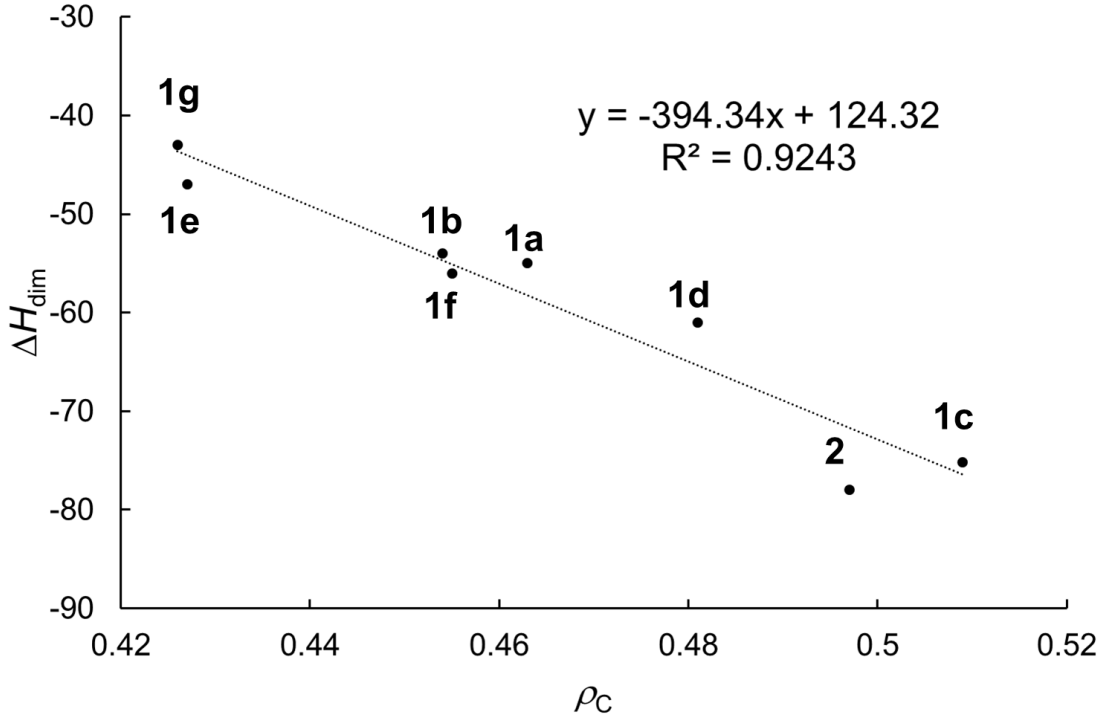

Figure S9. Plot of DFT-calculated ρ_c versus experimentally obtained ΔH_{dim}.

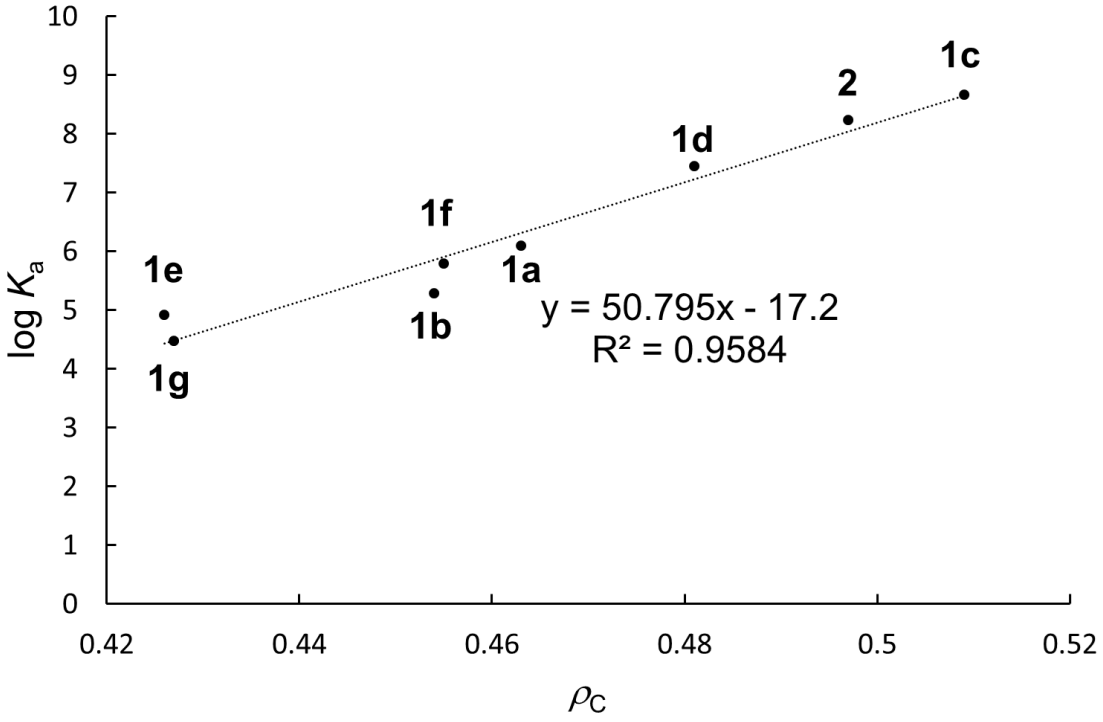

Figure S10. Plot of DFT-calculated ρ_c versus experimentally obtained association constants in a log scale.

Table S3: Thermodynamic parameters and DFT-calculated ρ_c of dicyanomethyl radicals.

	ρ_c	ΔH_{dim} / kJ mol^{-1}	ΔS_{dim} / J K^{-1} mol^{-1}	K_a (at 298 K)
1a•[S4]	0.463	-55	-68	1.26×10^6
1b•[S5]	0.454	-54	-80	1.93×10^5
1c•[S4]	0.509	-75	-86	4.71×10^8
1d•[S5]	0.481	-61	-62	2.84×10^7
1e•[S6]	0.427	-47	-72	3.00×10^4
1f•[S6]	0.455	-56	-77	6.22×10^5
1g•[S6]	0.426	-43	-50	8.42×10^4
2•	0.497	-78	-104	1.74×10^8

[S4] T. Kobashi, D. Sakamaki, S. Seki, *Angew. Chem. Int. Ed*. 2016, **55**, 8634.

[S5] K. Okino, S. Hira, Y. Inoue, D. Sakamaki, S. Seki, *Angew. Chem. Int. Ed*. 2017, **56**, 16597.

[S6] K. Okino, D. Sakamaki, S. Seki, *ACS Materials Lett.* 2019, **1**, 25.

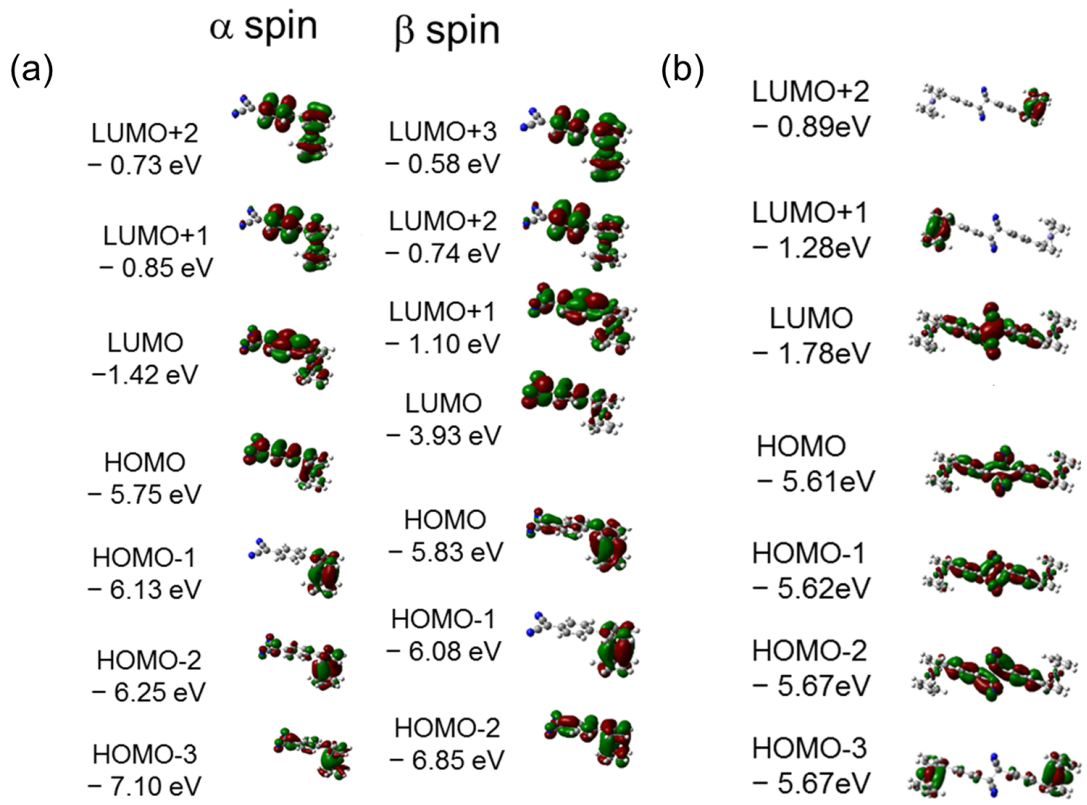

Figure S11. Frontier Kohn-Sham MOs of (a) **2•** and (b) **2**$_2$ at the (U)B3LYP/6-31G(d) (for C, H, N), LANL2DZ (for Fe) level of theory.

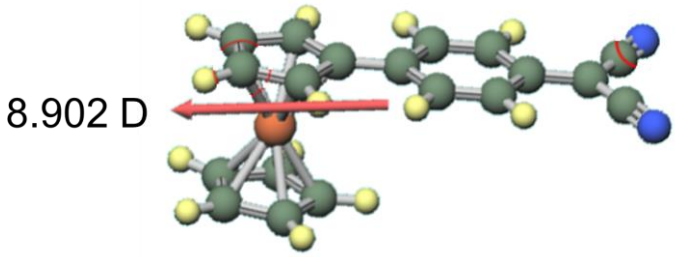

Figure S12. Calculated dipole moment of **2•** at the UB3LYP/6-31G(d) (for C, H, N), LANL2DZ (for Fe) level of theory.

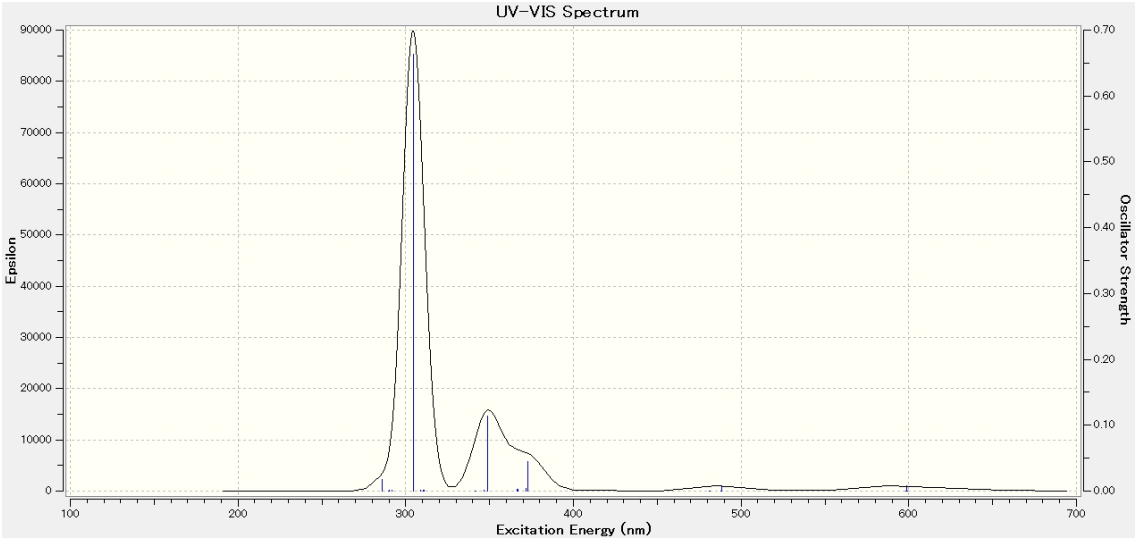

Figure S13. TD-DFT simulated electronic absorption spectrum of $\mathbf{2_2}$ calculated at B3LYP/6-31G(d) and LanL2DZ level of theory.

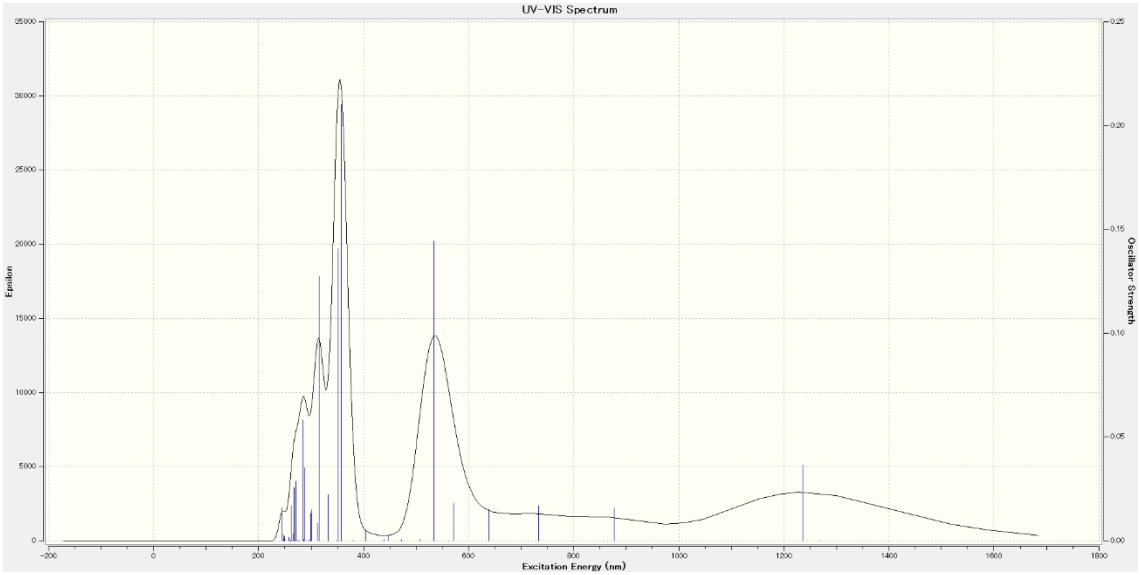

Figure S14. TD-DFT simulated electronic absorption spectrum of **2•** calculated at UB3LYP/6-31G(d) and LanL2DZ level of theory.

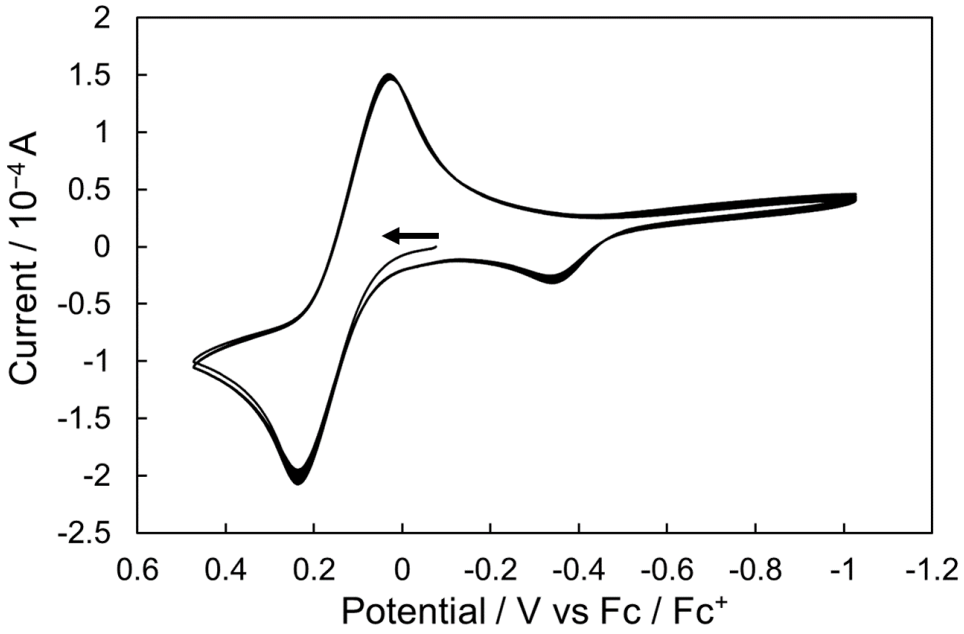

Figure S15. Cyclic voltammogram of **2₂** (10 cycles) in dichloromethane at 291 K (scan rate = 100 mV s^{-1}) with the 0.1 M *n*Bu_4NBF_4 electrolyte.

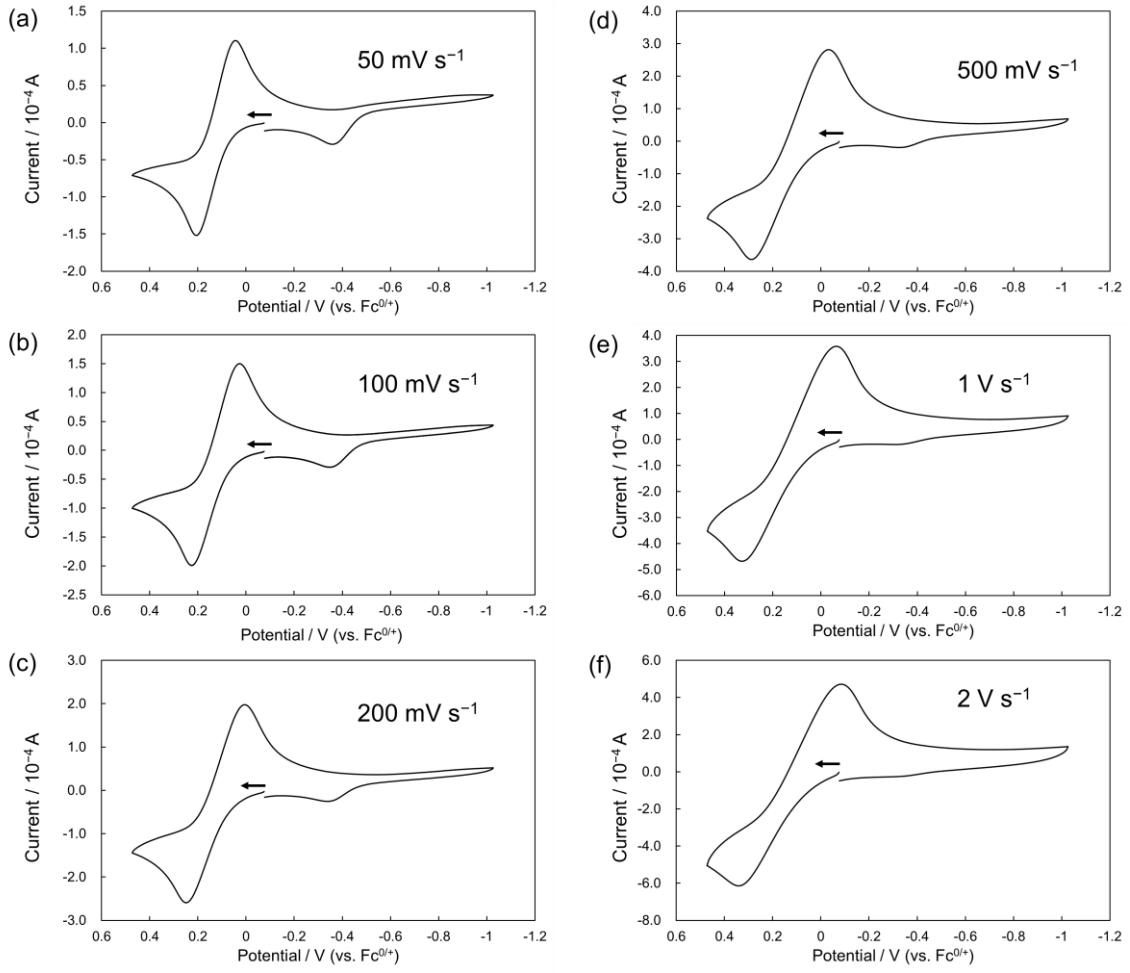

Figure S16. Scan rate dependence of cyclic voltammogram of **2₂** in dichloromethane at 291 K with the 0.1 M nBu$_4$NBF$_4$ electrolyte.

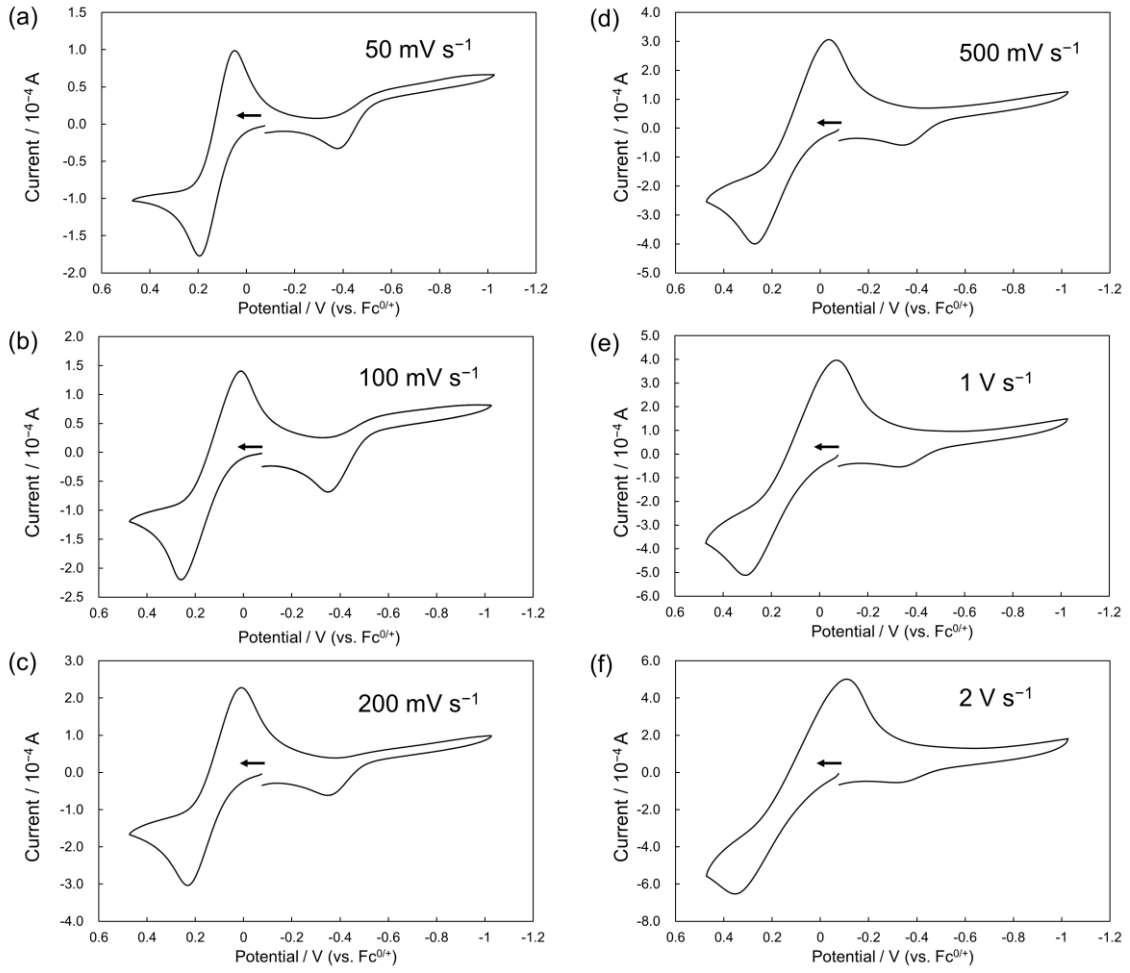

Figure S17. Scan rate dependence of cyclic voltammogram of **2**$_2$ in dichloromethane at 308 K with the 0.1 M nBu$_4$NBF$_4$ electrolyte.

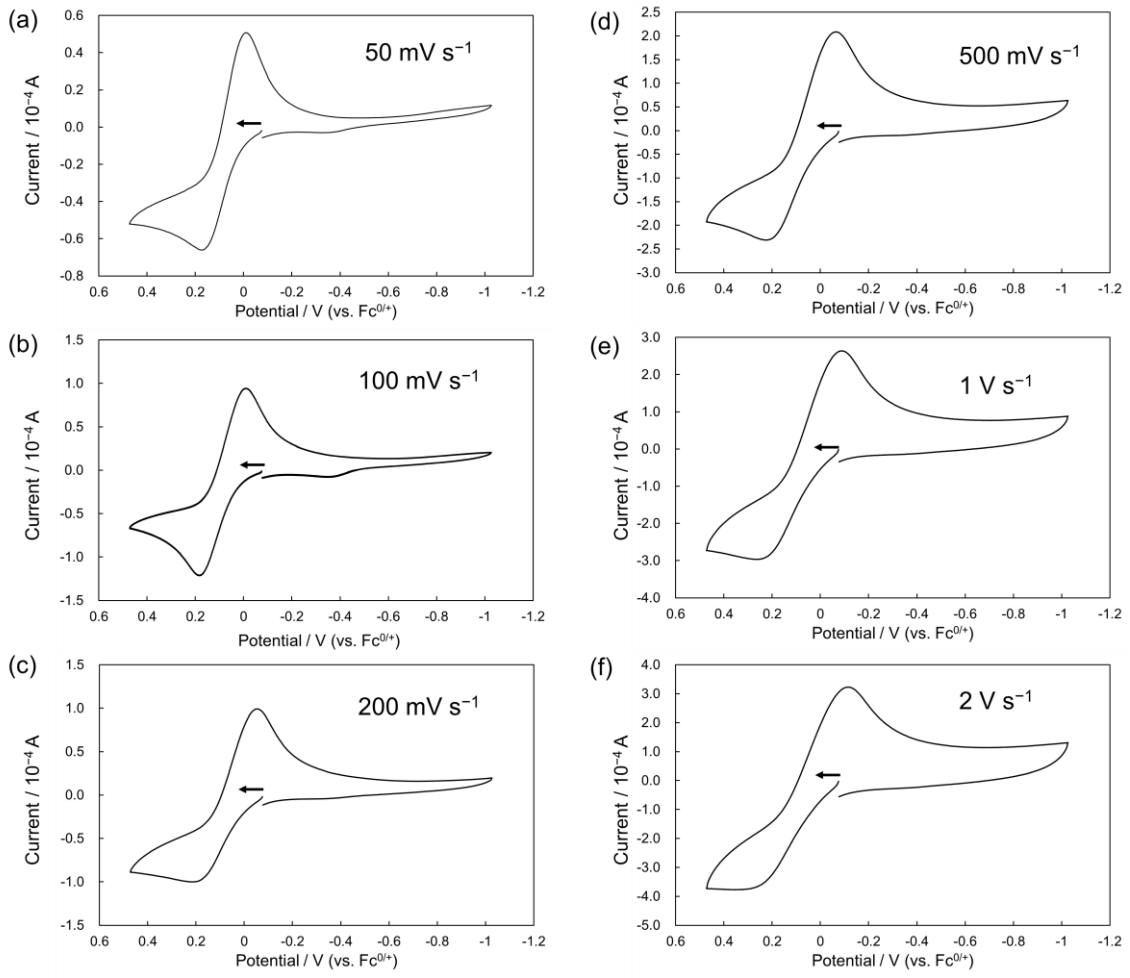

Figure S18. Scan rate dependence of cyclic voltammogram of **2₂** in dichloromethane at 273 K with the 0.1 M nBu$_4$NBF$_4$ electrolyte.

DFT-optimized geometries and energies

2• at the UB3LYP/6-31G(d) (for C, H, N), LANL2DZ (for Fe) level of theory

E(UB3LYP) = -964.721008867

C 3.093866 -1.863325 -0.590691
C 1.788257 -1.869053 -0.027097
C 3.094056 -0.965460 -1.699497
C 0.948150 -0.986405 -0.798891
C 1.788593 -0.415106 -1.822509
H 3.946502 -2.414888 -0.217682
H 1.486441 -2.440493 0.839509
H 3.946904 -0.715314 -2.316290
C -0.462741 -0.691057 -0.559938
H 1.487053 0.313176 -2.562318
C 3.967267 1.565566 0.346450
C 3.971955 0.666539 1.454127
C 2.657945 2.126778 0.238500
C 2.665474 0.670957 2.032140
C 1.856209 1.576436 1.282847
H 4.800262 1.763158 -0.315319
H 4.808889 0.062520 1.779053
H 2.326108 2.827590 -0.516042
H 2.340222 0.075148 2.874654
H 0.804711 1.772810 1.446740
Fe 2.565277 0.052956 0.043169
C -1.178334 -1.315216 0.490182
C -1.174515 0.217333 -1.380105
C -2.508327 0.496132 -1.163322
C -2.512169 -1.045094 0.717744
C -3.220061 -0.126108 -0.102650
H -0.666031 0.708886 -2.202842
H -3.025850 1.197713 -1.810451
H -0.673097 -2.027000 1.134524
H -3.032734 -1.540786 1.531450
C -4.604935 0.162134 0.130654
C -5.320683 -0.453273 1.187320
C -5.317103 1.077788 -0.682950

N -5.892254 -0.970574 2.064676

N -5.885462 1.836751 -1.364857

Major transitions of **2**• (f > 0.01)

Excited State 2: 2.582-A 1.0034 eV 1235.58 nm f=0.0363 <S**2>=1.416

77A -> 80A	0.21282
77A -> 83A	0.18383
79A -> 80A	0.18598
77B -> 81B	0.15732
78B -> 79B	0.77936
78B -> 80B	-0.40502
78B -> 83B	-0.29208
78B <- 80B	-0.10196

Excited State 3: 3.290-A 1.4132 eV 877.32 nm f=0.0158 <S**2>=2.455

77A -> 80A	0.18195
77A -> 83A	0.20602
78A -> 81A	-0.43315
78A -> 82A	-0.49025
77B -> 81B	0.51322
77B -> 82B	0.29013
78B -> 79B	-0.38384
78B -> 83B	-0.12376
78A <- 81A	-0.10964
78A <- 82A	-0.12471
77B <- 81B	0.12876

Excited State 5: 3.140-A 1.6905 eV 733.42 nm f=0.0169 <S**2>=2.214

75A -> 80A	0.10366
75A -> 83A	0.11916
76A -> 80A	0.15693
76A -> 83A	0.15347
77A -> 80A	-0.35535
77A -> 83A	-0.37060
78A -> 81A	-0.12499
78A -> 82A	-0.15039
79A -> 80A	-0.18042

79A -> 83A -0.18051
75B -> 79B 0.20347
75B -> 80B -0.20654
75B -> 83B -0.18147
76B -> 79B 0.16291
77B -> 81B 0.27901
77B -> 82B 0.15301
78B -> 79B 0.39661
78B -> 80B 0.27583
78B -> 83B 0.29412

Excited State 7: 2.881-A 1.9447 eV 637.54 nm f=0.0152 <S**2>=1.825
75A -> 80A 0.10179
76A -> 80A 0.16585
76A -> 83A 0.16082
77A -> 80A 0.22899
77A -> 83A 0.21191
78A -> 81A 0.16089
78A -> 82A 0.18623
75B -> 79B 0.53060
75B -> 80B -0.38583
75B -> 83B -0.29336
76B -> 79B 0.35030
76B -> 80B -0.18479
76B -> 83B -0.14793
77B -> 81B -0.16180
78B -> 79B -0.11089
78B -> 80B -0.10728
78B -> 83B -0.10037

Excited State 8: 2.069-A 2.1716 eV 570.94 nm f=0.0180 <S**2>=0.820
77A -> 80A 0.26475
77A -> 83A 0.26443
78A -> 81A -0.28183
78A -> 82A -0.32056
79A -> 80A 0.23752
79A -> 83A 0.10081

76B -> 79B -0.19430
77B -> 81B -0.38425
77B -> 82B -0.21264
78B -> 79B 0.21276
78B -> 80B 0.41107
78B -> 83B 0.37459

Excited State 11: 2.116-A 2.3243 eV 533.42 nm f=0.1442 <S**2>=0.869
77A -> 80A 0.10571
78A -> 81A -0.13605
78A -> 82A -0.15413
79A -> 80A -0.17557
79A -> 83A 0.11168
72B -> 79B -0.11462
75B -> 79B -0.33490
75B -> 80B 0.12007
76B -> 79B 0.83849
77B -> 81B -0.12654

2$_2$ at the B3LYP/6-31G(d) (for C, H, N), LANL2DZ (for Fe) level of theory

E(RB3LYP) = -1929.45237171

C	-8.13598	2.03608	0.35223
C	-6.81662	1.73599	0.79594
C	-8.25396	1.60911	-1.00412
C	-6.09583	1.12645	-0.28955
C	-7.0064	1.04761	-1.39927
H	-8.91959	2.48057	0.95128
H	-6.42588	1.93722	1.78404
H	-9.1459	1.66358	-1.61401
C	-4.69322	0.67758	-0.27149
H	-6.79682	0.60186	-2.36208
C	-9.2291	-1.00671	1.31968
C	-7.93383	-1.28102	1.85505
C	-9.24996	-1.45444	-0.03578

C	-7.155	-1.89821	0.83013
C	-7.9677	-2.00556	-0.33869
H	-10.04113	-0.51535	1.83949
H	-7.59415	-1.03842	2.85342
H	-10.08012	-1.36005	-0.72337
H	-6.11694	-2.19311	0.9111
H	-7.65605	-2.40502	-1.2947
Fe	-7.77407	-0.00991	0.21428
C	-3.99122	0.50928	0.93557
C	-4.00282	0.41159	-1.46632
C	-2.68016	-0.01953	-1.45987
C	-2.6665	0.08849	0.95136
C	-1.99553	-0.1826	-0.24903
H	-4.50177	0.54952	-2.41993
H	-2.18639	-0.22535	-2.40382
H	-4.49096	0.693	1.8811
H	-2.16254	-0.03798	1.90388
C	-0.52008	-0.61947	-0.24048
C	-0.19584	-1.35173	0.99919
C	-0.23553	-1.51766	-1.37661
C	8.08387	-2.06043	0.45927
C	6.76789	-1.70593	0.87232
C	8.22698	-1.70397	-0.91521
C	6.07527	-1.1334	-0.25066
C	6.99763	-1.13334	-1.35272
H	8.84952	-2.49459	1.08836
H	6.35762	-1.85119	1.86252
H	9.12356	-1.81111	-1.51109
C	4.68117	-0.65962	-0.27168
H	6.80727	-0.72984	-2.33809
C	9.29536	1.37394	-0.08154
C	9.24474	0.99294	1.2934
C	8.03303	1.94495	-0.42839
C	7.95078	1.32793	1.79669
C	7.20288	1.91677	0.73266
H	10.13088	1.22339	-0.75244

H	10.03566	0.50438	1.84725
H	7.74498	2.30606	-1.4068
H	7.59189	1.14281	2.80065
H	6.17261	2.24392	0.78526
Fe	7.7769	-0.01573	0.21735
C	4.00253	-0.32543	0.91376
C	3.97586	-0.54255	-1.48096
C	2.65646	-0.10115	-1.51107
C	2.68191	0.10741	0.89428
C	1.99322	0.22358	-0.32136
H	4.45945	-0.81201	-2.41435
H	2.14825	-0.01646	-2.4659
H	4.5207	-0.38659	1.86536
H	2.19442	0.36441	1.82894
C	0.51838	0.6623	-0.34437
C	0.21999	1.56477	0.7847
C	0.20762	1.38871	-1.59083
N	0.00236	2.26239	1.68517
N	-0.01794	1.94747	-2.58171
N	-0.03109	-2.21291	-2.28203
N	0.04183	-1.91458	1.98487

Major transitions of **2₂** (*f* > 0.01)

Excited State 9:	Singlet-A	3.3277 eV	372.58 nm	f=0.0453	<S**2>=0.000
150 ->158	0.11057				
150 ->159	0.15389				
150 ->160	0.10992				
150 ->161	-0.11027				
150 ->167	0.20035				
150 ->168	-0.10903				
151 ->158	0.10710				
151 ->160	0.10603				
151 ->168	-0.11344				
154 ->164	-0.18412				
154 ->165	-0.16736				
156 ->158	0.15172				

156 ->159	0.13119				
157 ->158	0.40500				
Excited State 13:	Singlet-A	3.5530 eV	348.96 nm	f=0.1137	<S**2>=0.000
153 ->158	-0.10250				
155 ->164	0.10885				
155 ->165	-0.11504				
156 ->159	-0.13895				
156 ->167	-0.18650				
157 ->158	0.48432				
157 ->160	-0.16004				
157 ->166	-0.12182				
157 ->168	0.14596				
Excited State 21:	Singlet-A	4.0736 eV	304.36 nm	f=0.6633	<S**2>=0.000
153 ->158	0.65348				
156 ->159	-0.20627				
Excited State 25:	Singlet-A	4.3391 eV	285.73 nm	f=0.0172	<S**2>=0.000
154 ->162	0.10065				
155 ->161	0.16878				
155 ->162	0.37489				
155 ->163	0.31070				
156 ->161	0.14939				
156 ->167	0.10678				
157 ->160	-0.30376				